Laser-Induced Mouse Model of Chronic Ocular Hypertension

Sinisa D. Grozdanic,[1,2] *Daniel M. Betts,*[1] *Donald S. Sakaguchi,*[2,3] *Rachell A. Allbaugh,*[2] *Young H. Kwon,*[4] *and Randy H. Kardon*[4]

Purpose. To develop an inducible mouse model of glaucoma.

Methods. An obstruction of aqueous humor outflow in adult C57BL6/J mice was induced by combined injection of indocyanine green (ICG) dye into the anterior chamber and diode laser treatment. To evaluate intraocular pressure (IOP), tonometry was performed with a modified Goldmann tonometer. The function of the retina was evaluated with electroretinography (ERG).

Results. IOP was significantly elevated in surgical eyes compared with control eyes: before surgery, 15.2 ± 0.6 mm Hg; 10 days after surgery, 33.6 ± 1.5 mm Hg ($P < 0.001$); and 30 days after surgery, 27.4 ± 1.2 mm Hg ($P < 0.001$). However, 60 days after surgery, IOP in the surgical eyes decreased to 19.5 ± 0.9 mm Hg and was not significantly different compared with control eyes (control, 17.3 ± 0.7 mm Hg; $P = 0.053$). ERG amplitudes, expressed as a ratio (surgical/control), were decreased in surgical eyes. The amplitudes for b-wave were: before surgery, 107.6% ± 4.6%; 28 days after surgery, 61% ± 4% ($P < 0.001$); and 56 days after surgery, 62% ± 5.6% ($P < 0.001$). Oscillatory potentials were the most dramatically affected: before surgery, 108.6% ± 6.7%; 28 days after surgery, 57.5% ± 5% ($P < 0.01$); and 56 days after surgery, 57% ± 8.5% ($P < 0.001$). Amplitudes of the a-waves had relatively smaller but still significant deficits: before surgery, 105.8% ± 6.9%; 28 days after surgery, 72.2% ± 5.4% ($P < 0.01$); and 56 days after surgery, 79.8% ± 11.0% ($P < 0.01$). Histologic analysis of the surgical eyes revealed development of anterior synechia, loss of retinal ganglion cells (RGCs), and thinning of all retinal layers. Electron microscopy of optic nerve cross sections revealed swelling and degeneration of the large diameter axons and gliosis.

Conclusions. Diode laser treatment of ICG saturated episcleral veins causes a chronic elevation of IOP and sustained ERG deficits. (*Invest Ophthalmol Vis Sci.* 2003;44:4337–4346) DOI: 10.1167/iovs.03-0015

Glaucoma is a progressive optic neuropathy with characteristic optic disc changes and progressive visual field defects.[1] The elevated intraocular pressure (IOP) is considered a primary risk factor for the initiation and progression of glaucomatous neuropathy.[2] However, in many patients, despite adequate control of IOP, the loss of vision continues to progress, which dictates the necessity for the further identification of molecular mechanisms responsible for glaucomatous neurodegeneration.[3]

Despite new discoveries, the genetic and environmental factors causing and modifying glaucoma have not been clearly defined.[4] Different molecular mediators have been proposed as potential suspects in glaucomatous neurodegeneration (inducible nitric oxide synthase [iNOS],[5–7] TNF-α,[8,9] lack of growth factors or their receptors,[10] and alteration of optic nerve head matrix molecules[11]). A disruption of adequate blood supply and energy metabolism[12–14] or dysfunctional protein secretion[15] have also been suggested to be causes of the selective death of retinal ganglion cells (RGCs) in glaucoma.

A potentially powerful model for the investigation of these factors is the mouse, in which the genome can readily be altered by adding, changing, or deleting genes.[16,17] However, the small size of the mouse eye has precluded noninvasive monitoring of IOP and optic nerve function, greatly restricting the use of a mouse model in glaucoma studies.[16]

A procedure for the reliable induction of chronic ocular hypertension in genetically manipulated mice may provide a unique advantage in the investigation of the link between other neurodegenerative diseases and glaucoma.[18–20] Furthermore, the availability of transgenic mice that mimic different human diseases could provide an opportunity to identify possible risk factors that may predispose to and/or are responsible for RGC death due to chronic elevation of IOP. The induction of chronic ocular hypertension in transgenic or knockout mice in which signaling molecules and/or their receptors are altered may offer a powerful tool for the investigation of signal transduction mechanisms involved in the RGC death that occurs in glaucoma.[17]

We recently adapted and validated noninvasive techniques currently used to study aqueous humor outflow properties (fluorophotometry),[21] tonometry, and retinal function[22] in small laboratory animals. The goal of this study was to investigate whether it is possible to induce reliably a chronic elevation of IOP in mice, evaluate potential functional deficits of the retina using electroretinography (ERG), and determine whether morphologic changes resemble changes in glaucomatous human eyes.

Materials and Methods

Laser Induction of Chronic Ocular Hypertension

All animal studies were conducted in accordance with the ARVO Statement for the Use of Animals in Ophthalmic and Vision Research,

From the Departments of [1]Veterinary Clinical Sciences and [2]Biomedical Sciences, College of Veterinary Medicine, and the [3]Department of Zoology and Genetics, Iowa State University, Ames, Iowa; and the [4]Department of Ophthalmology and Visual Sciences, University of Iowa Hospitals and Clinics, Iowa City, Iowa.

Supported by a Special Research Incentive Grant from the College of Veterinary Medicine, Iowa State University; funds from The Glaucoma Foundation; an unrestricted grant from Research to Prevent Blindness to the Department of Ophthalmology, University of Iowa; and a Merit Review Grant from the Veterans Administration (RHK). RHK is a Research to Prevent Blindness Lew Wasserman Scholar.

Submitted for publication January 6, 2003; revised April 24 and May 26, 2003; accepted June 3, 2003.

Disclosure: **S.D. Grozdanic**, Haag-Streit USA (F); **D.M. Betts**, None; **D.S. Sakaguchi**, None; **R.A. Allbaugh**, None; **Y.H. Kwon**, None; **R.H. Kardon**, None

The publication costs of this article were defrayed in part by page charge payment. This article must therefore be marked "*advertisement*" in accordance with 18 U.S.C. §1734 solely to indicate this fact.

Corresponding author: Sinisa D. Grozdanic, Department of Veterinary Clinical Sciences, College of Veterinary Medicine, Iowa State University, Ames, IA 50011; sgrozdan@iastate.edu.

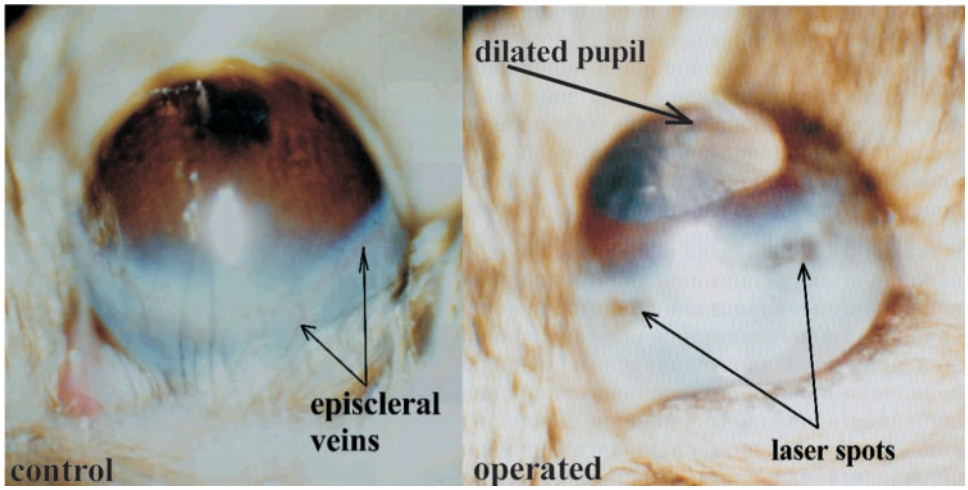

FIGURE 1. Laser surgery of the indocyanine green–pretreated eyes. *Right*: surgical eye of one animal 60 days after surgery. Laser spots are distributed over the episcleral vein regions. A mid-dilated and light-unresponsive pupil was evident in the surgical eye. *Left*: control eye (isoflurane anesthesia commonly induces pupil constriction).

and procedures were approved by the Iowa State University Committee on Animal Care. C57/BL6 mice (6–8 months of age, $n = 54$) were used in the experiments. Mice were kept in a 10:14-hour light–dark regimen.

Laser treatment of the trabecular meshwork in monkeys and rats produces chronic elevation of IOP.[23,24] We hypothesized that this would also be true of the mouse eye. We injected the photosensitive dye (indocyanine green) in the anterior chamber of one eye to increase the local photocoagulative effect of the laser treatment.

Briefly, mice were anesthetized with 2.5% isoflurane+100% oxygen, and body temperature was maintained with a heating pad. Indocyanine green (3 μL, 10 mg/mL; Sigma-Aldrich, St. Louis, MO) was injected into the anterior chamber of the eye at a very slow rate with a syringe (Hamilton, Reno, NV) attached to a microinjector pump, to avoid an abrupt elevation of IOP during the procedure. Animals were pretreated with 4% pilocarpine hydrochloride eye drops, which increased outflow of the dye into the trabecular meshwork and episcleral veins. The pilocarpine treatment also caused miosis, which served to protect the posterior pigmented structures of the eye from the diode laser energy (the pigmented iris served as a barrier for any potential stray energy). Twenty minutes after injection, a diode laser (DioVet; Iridex Corp., Mountain View, CA) was used to deliver 810-nm energy pulses through a 50-μm fiberoptic probe to the region of the trabecular meshwork and episcleral veins in proximity to the limbal region. Careful positioning of the fiberoptic probe insured that the orientation of the laser was away from the pigmented structures of the retina. We delivered between 30 and 50 laser spots exteriorly over a 300° range of the limbal radius (350 mW energy, 1500-ms pulse duration; Fig. 1). After surgery, pain was controlled by acetaminophen (100 mg/kg) and codeine (75 mg/kg) in the drinking water for 7 days. To prevent potential infection, antibiotic ointment (neomycin+polymyxin B bacitracin; Bausch & Lomb Pharmaceuticals, Inc., Tampa, FL) was applied topically after the procedure.

IOP Monitoring

IOP was measured with a modified Goldmann tonometer (Haag-Streit USA, Inc., Mason, OH), as previously described (Fig. 2).[22,25] Tonometry in mice required a modified applanation prism with a biprism angle of 36° and applied weight of 25 mg per scale division (2 g full scale), as previously described by Cohan and Bohr.[25] A calibration of the modified Goldmann tonometer was performed by comparing IOP results measured by invasive manometry and modified tonometry ($y = 1.74 \pm 0.97x$, $r^2 = 0.89$).[22]

IOPs were measured in anesthetized mice, under 1% halothane and 30% NO-70% O_2 anesthesia. The Goldmann tonometer tip was applied toward the center of the cornea, and 5 to 10 readings were obtained for the calculation of mean pressures in each eye.

Fluorophotometric Evaluation of Aqueous Humor Flow

Fluorophotometry was pioneered by Goldmann[26] as an objective method to measure aqueous humor flow by measuring the rate of clearance of fluorescein from the anterior chamber. It has been demonstrated that the aqueous flow and fluorescein clearance are decreased in monkeys with laser-induced chronic ocular hypertension.[27] Thus, we were interested in determining whether that is the case in laser-treated mouse eyes as well.

Iontophoretic Application of Fluorescein. Fluorescein was applied to the anterior chamber of the mouse eye by iontophoresis, as we have described.[21] Briefly, uniform (0.465 g) blocks of 2% agarose gel containing 0.5% fluorescein (AK-Fluor; Akorn, Inc., Decatur IL) were placed on the cornea. The gels were held in position by a syringe filled with 0.9% saline, containing the negative electrode of an iontophoretic device (Phoresor II; Motion Control Inc., Salt Lake City, UT). The positive electrode of this device was placed on the occipital

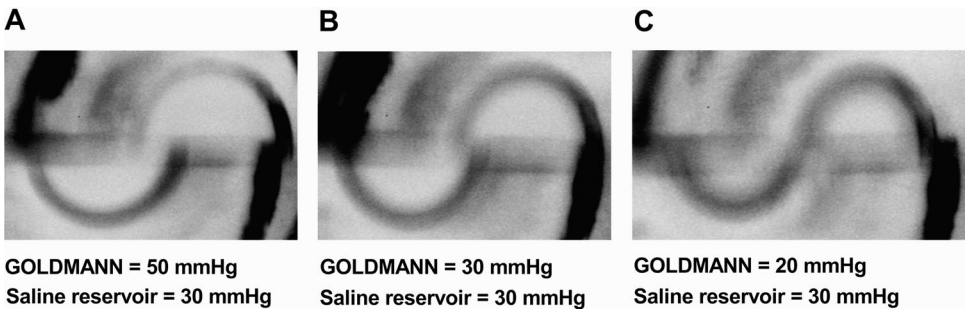

FIGURE 2. Goldmann tonometer recording procedure in a mouse. A 25-gauge needle connected to a reservoir containing 0.9% NaCl was carefully inserted in the posterior chamber, and IOP was then raised to 30 mm Hg by elevating the reservoir. (**A**) The Goldmann tonometer scale was set at 50 mm Hg. (**B**) Reading from the Goldmann tonometer was obtained when fluorescent rings reached a matching position (reading was 30 mm Hg, which corresponded well to the preset IOP value). (**C**) The Goldmann tonometer scale was set on 20 mm Hg (fluorescent rings do not overlap). Images were obtained with a video camera attached to the slit lamp biomicroscope in which the optical axis was aligned with the optic prism.

region of the anesthetized animal, and a 2.5-mA current applied for 5 minutes. Fluorescein is a negatively charged molecule and can diffuse through the electrical gradient toward the positive electrode. The Phoresor II has the capability of automatically stopping the current and time countdown if corneal contact with the gel is lost, ensuring that a constant amount of fluorescein is delivered during iontophoresis.

Fluorophotometry. Fluorophotometry was performed with a slit lamp biomicroscope equipped with a high integration charge coupled device (Cohu, San Diego, CA) attached to a bioimage analysis system (model 500; Bioimage Co., Chicago, IL) that can detect low-level fluorescence. The images were digitized and the optic density quantified with image-analysis software (Scion Corp., Frederick, MD). Excitation of fluorescein was achieved with a cobalt blue filter. A barrier filter (Wratten filter no. 15; Kodak film tablet; Eastman Kodak Co., Rochester, NY) was used for the selective detection of fluorescence from the anterior chamber. Baseline fluorescence was measured, and system calibration was performed in each animal by using the calibrated gray scale (Kodak film tablet; Eastman Kodak Co.) as a standard before application of fluorescein. Fluorescence was measured at 15-minute intervals for 160 minutes after application of fluorescein. Fluorescein clearance was calculated using the published formula[28]: $Cl = (A - B)/[(A + B)/2] \cdot t_{int}$, where Cl is clearance, A is fluorescence at time point A, B is fluorescence at time point B; and t_{int} is the time interval between points A and B.

Electroretinography

Electroretinography was used to determine physiological amplitudes and latencies of the retinal responses in 22 mice. Animals were dark adapted for at least 6 hours before each experiment. The animals were anesthetized as previously described, and the pupils dilated with 1% tropicamide and 2.5% phenylephrine. Mice were placed in a specially designed dome with an interior that was completely covered with aluminum foil to obtain a Ganzfeld effect. Body temperature was maintained with a microwave-heated thermal pad. A light stimulus was delivered through the ceiling of the dome (PS-22 stimulator; Grass-Telefactor, West Warwick, RI). Measured luminance in all quadrants was 1600 ± 200 cd/m^2. Two electrodes made of a DTL fiber (Chieldex Trading GmbH, Palmyra, NY) and Ag-AgCl cells were used to simultaneously record electroretinograms from both eyes. The reference electrode was positioned in the ear, and the ground electrode was placed subcutaneously on the back. An evoked potential measuring system (Neuropack-MEB 7102; Nihon-Kohden America, Foothill Ranch, CA) was used to deliver a triggered output to the flash stimulator and collect signals from both eyes. A flash ERG routine was delivered at a 0.2-Hz frequency (10 averaged signals per recording session, sensitivity 100 μV/division, low-cut frequency 0.5 Hz, high-cut frequency 10 kHz, analysis time 500 ms). Oscillatory potentials (OPs) were recorded by delivering light stimuli at a 0.2-Hz frequency (10 averaged signals per recording session, sensitivity 100 μV/division, low-cut frequency 50 Hz, high-cut frequency 500 Hz, analysis time 100 ms). Isolated cone responses were recorded from light-adapted eyes by delivering stimuli at 20 Hz (50 averaged signals per recording session, sensitivity 50 μV/division, low-cut frequency 0.5 Hz, high-cut frequency 10 kHz, analysis time 500 ms). To avoid potential bias due to electrode differences, recordings were repeated with electrodes switched to the opposite eyes.

Histologic Examination

Sixty-five days after surgery, mice were deeply anesthetized with a high dose of phenobarbital (100 mg/kg) and perfused intracardially with ice-cold heparinized saline followed by 4% paraformaldehyde in 0.1 M phosphate buffer. Optic nerves (dissected 1 mm posterior to the sclera) were postfixed in a solution containing 4% paraformaldehyde-2% glutaraldehyde in 0.1 M phosphate buffer (pH 7.4) and then rinsed in cacodylate buffer, postfixed in 2% osmium tetroxide in cacodylate buffer, dehydrated in alcohol, and embedded in epoxy resin. Cross sections (1 μm thick) were cut with an ultramicrotome, mounted on glass slides, and stained with 1% toluidine blue. Ultrathin sections of the optic nerves were examined by electron microscopy. Eye globes were paraffin embedded, and 7-μm-thick sections of the retina were collected onto poly-L-lysine–coated glass slides, and stained with hematoxylin and eosin. The eye globe tissue sections were examined with a photomicroscope (Microphot FXA; Nikon Corp., New York, NY). Images were captured with a digital camera (Megaplus model 1.4; Eastman Kodak Corp.) connected to a framegrabber (MegaGrabber; Eastman Kodak Corp.) in a computer (Macintosh 8100/80 AV; Apple Computer, Cupertino, CA) using NIH Image 1.58 VDM software (available by ftp at zippy.nimh.nih.gov/ or at http://rsb.info.nih.gov/nih-image; developed by Wayne Rasband, National Institutes of Health, Bethesda, MD).

The morphometric analysis of the retina was performed as we have described.[29] Briefly, sections of the retina at the level of the optic nerve head were prepared, and each section was divided into 12 optic fields (6 fields of the central retina and 6 fields of the peripheral retina). Within each field we measured the thickness of the inner plexiform and RGC layer (IPL+RGC), inner nuclear (INL), and outer nuclear layer (ONL) by measuring each layer in four places and calculating the average thickness per section. Measurements of retinal layer thickness were performed using a calibrated scale of the objective of the light microscope.

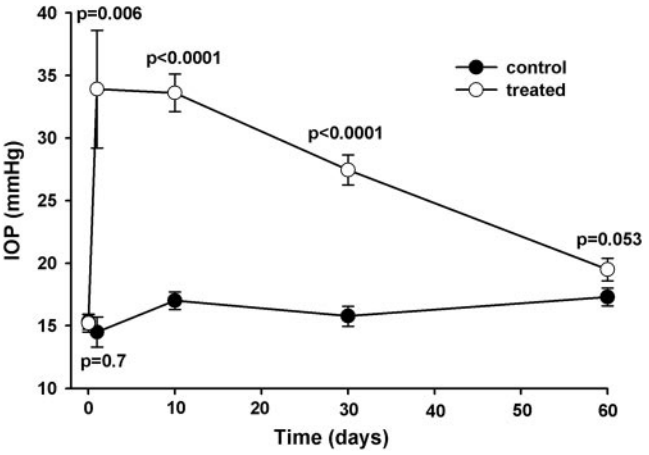

FIGURE 3. Tonometry data in surgically treated mice. Laser treatment of indocyanine green–pretreated eyes induced elevation of IOP at 1, 10, and 30 days, but not 60 days, after surgery. Data are the mean ± SEM.

Statistical Analysis

Statistical analysis was performed by Student's *t*-test, a paired *t*-test, the Kruskal-Wallis nonparametric test, and correlation analysis performed on computer (GraphPad, San Diego, CA).

RESULTS

Tonometry and Fluorophotometry

IOP was significantly elevated in eyes of 22 (88%) of 25 surgically altered mice after laser-induced surgery compared with control (nonsurgical) eyes (Fig. 3).

Preoperative IOPs (n = 22) were 15.2 ± 0.6 mm Hg (left eyes) and 15.3 ± 0.6 mm Hg (right eyes); 12 hours after surgery, 33.9 ± 4.7 mm Hg (left eyes-surgical) and 14.5 ± 1.2 mm Hg (right eyes-control; $P = 0.006$, paired *t*-test; $n = 6$); 10 days after surgery, 33.6 ± 1.5 mm Hg (surgical eyes) and 17 ± 0.7 mm Hg (control eyes; $P < 0.001$, paired *t*-test; $n = 22$); and 30 days after surgery, 27.4 ± 1.2 mm Hg (surgical) and 15.8 ± 0.8 (control; $P < 0.001$, paired *t*-test, $n = 22$). However, 60 days after surgery IOP in the surgical eyes decreased to 19.5 ±

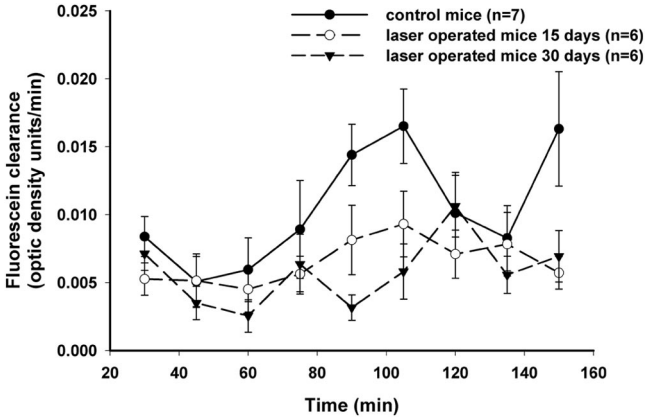

FIGURE 4. Fluorophotometry analysis revealed decreased fluorescein clearance in surgical eyes compared with healthy, nonsurgical control eyes. Data are the mean ± SEM.

0.9 mm Hg and was not significantly different than in control eyes (control, 17.3 ± 0.7 mm Hg; $P = 0.053$, paired *t*-test, $n = 21$). To evaluate whether laser treatment induced an immediate elevation of IOP and to rule out the possibility that we had an immediate spike in IOP that might cause absolute retinal ischemia, six mice were operated on, and IOP was evaluated 12 hours after surgery. IOP was significantly elevated in the surgical eyes (33.9 ± 4.7 mm Hg, $P = 0.006$, paired *t*-test) when compared with the control eyes (14.5 ± 1.2 mm Hg). Only one animal had IOP above 40 mm Hg (45 mm Hg). Immediate recording of IOP was not possible, because of the aqueous humor leak from the needle track that was created during the injection of indocyanine green dye.

An analysis of the fluorophotometry data (Fig. 4) revealed significantly decreased fluorescein clearance in surgical eyes at 15 ($P = 0.02$, Student's *t*-test) and 30 ($P = 0.01$, Student's *t*-test) days after surgery.

Electroretinography

Electroretinography was used as an objective method to evaluate the functional status of the inner and outer retina. To evaluate the effect of the chronic elevation of IOP on different populations of photoreceptors, we used full-field scotopic flash ERG to evaluate combined rod and cone activity and photopic flicker ERG (flERG) for the isolated cone activity.

ERG amplitudes, expressed as a ratio (surgical/control), were decreased in surgical eyes, and retinal inner function was predominantly affected (Fig. 5).

The amplitudes of a-waves (Fig. 6A) had relatively smaller but still significant deficits compared with b-waves and OPs: control, 105.8% ± 6.9%; 28 days after surgery, 72.2% ± 5.4% ($P < 0.01$, Kruskal-Wallis nonparametric test with the Dunn post test), and 56 days after surgery, 79.8% ± 11% ($P < 0.01$, Kruskal-Wallis nonparametric test with the Dunn post test). flERG analysis (Fig. 6B) revealed a mild but nonsignificant decrease of the function in surgical eyes: control, 99% ± 9%; 28 days after surgery, 78.5% ± 13.3% ($P > 0.1$, Kruskal-Wallis nonparametric test with the Dunn post test), and 56 days after surgery, 88.3% ± 13.3% ($P > 0.1$, Kruskal-Wallis nonparametric test with the Dunn post test). However, when absolute amplitudes were compared between surgical and control (nonsurgical) eyes there was a significant decrease in surgical eyes at 28 ($P = 0.001$, paired *t*-test) but not at 56 ($P = 0.3$, paired *t*-test) days after surgery. The amplitudes for b-wave (Fig. 6C) were control, 107.6% ± 4.6%, and 28 days after surgery, 61% ± 4% ($P < 0.001$, Kruskal-Wallis nonparametric test with the Dunn post test; $n = 22$); 56 days after surgery, 62% ± 5.6% ($P < 0.001$, Kruskal-Wallis nonparametric test with the Dunn post test). OPs were the most dramatically affected (Fig. 6D): control, 108.6% ± 6.7%; 28 days after surgery, 57.5% ± 5% ($P < 0.01$, Kruskal-Wallis nonparametric test with the Dunn post test); and 56 days after surgery, 57% ± 8.5% ($P < 0.001$, Kruskal-Wallis nonparametric test with the Dunn post test).

The latency of flERG responses, b-waves, and OPs was significantly increased in surgical eyes 28 days after surgery (Fig. 7): a-wave $\text{latency}_{\text{control}}$, 22.2 ± 0.7 ms, and $\text{latency}_{\text{surgical}}$, 23 ± 0.7 ms ($P = 0.06$, paired *t*-test); b-wave $\text{latency}_{\text{control}}$, 19.6 ± 0.4, and $\text{latency}_{\text{surgical}}$, 22 ± 0.9 ms ($P = 0.03$, paired *t*-test); OPs $\text{latency}_{\text{control}}$, 25.2 ± 0.9 ms, and $\text{latency}_{\text{surgical}}$, 26.5 ± 0.8 ms ($P = 0.04$, paired *t*-test); and flERG $\text{latency}_{\text{control}}$, 50.6 ± 1.5 ms, and $\text{latency}_{\text{surgical}}$, 53.9 ± 1.5 ms ($P = 0.03$, paired *t*-test).

However, when latencies were analyzed 56 days after surgery, only b-wave latencies of surgical eyes were significantly increased compared with control (nonsurgical) eyes: a-wave

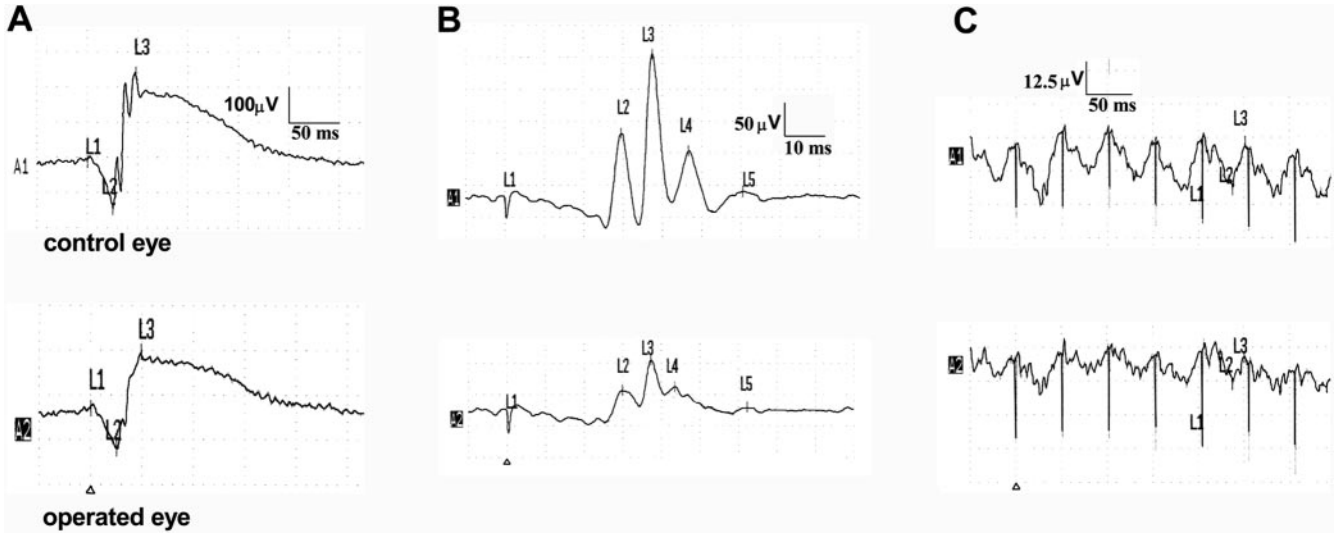

FIGURE 5. Original ERG traces from one of the surgically treated mice 56 days after surgery. (**A**) Scotopic flash ERG, (**B**) scotopic OPs, (**C**) photopic flERG. Laser-induced surgery was characterized by relatively nonaffected a-wave amplitudes (scotopic flash ERG) and photopic flicker ERG amplitudes; however, oscillatory potentials had dramatic deficits, which imply primary damage to the inner retina.

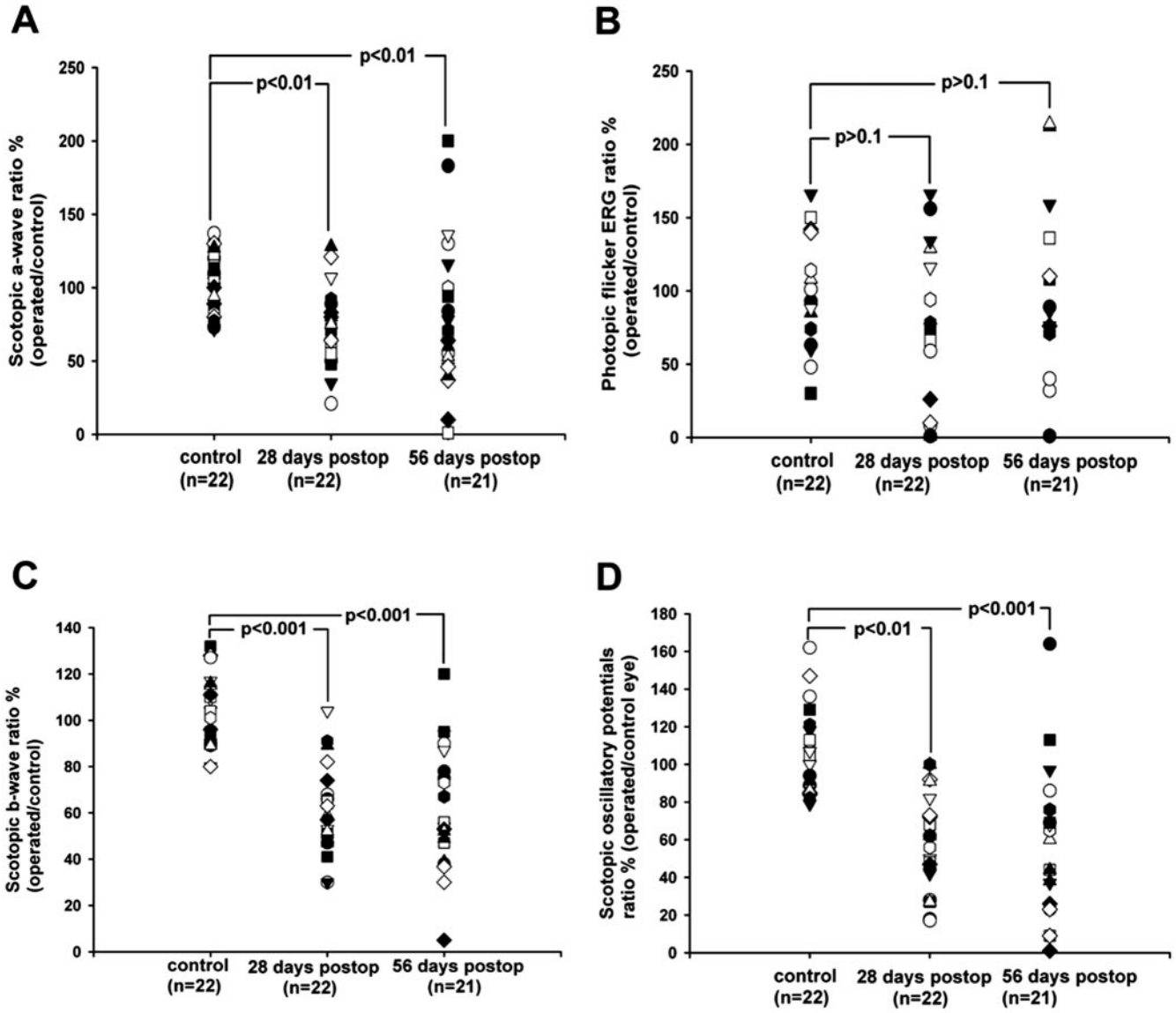

FIGURE 6. ERG amplitudes represented as a ratio (surgical/control). (**A**) Scotopic flash ERG a-wave, (**B**) photopic flicker ERG, (**C**) scotopic flash ERG b-wave, (**D**) scotopic OPs

$\text{latency}_{\text{control}}$, 23.5 ± 0.9 ms, and $\text{latency}_{\text{surgical}}$, 24.2 ± 1 ms ($P = 0.5$, paired *t*-test); b-wave $\text{latency}_{\text{control}}$, 15.7 ± 0.9, and $\text{latency}_{\text{surgical}}$, 20 ± 1.7 ms ($P = 0.02$, paired *t*-test); OPs $\text{latency}_{\text{control}}$, 28.2 ± 0.7 ms, and $\text{latency}_{\text{surgical}}$, 29.4 ± 1.3 ms ($P = 0.3$, paired *t*-test); and flERG $\text{latency}_{\text{control}}$, 49.7 ± 1.4 ms, and $\text{latency}_{\text{surgical}}$, 51.4 ± 1.9 ms ($P = 0.14$, paired *t*-test).

Because we were concerned that laser energy by itself or injection of the indocyanine green might cause retinal damage,

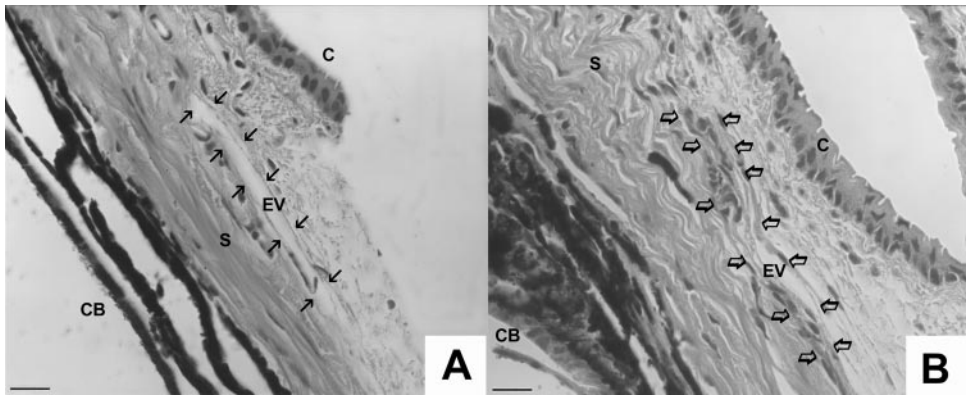

FIGURE 7. Laser cauterization of ICG-filled episcleral veins caused almost complete obstruction of the venous lumen. (**A**) Control. *Arrows*: borderlines of an episcleral vein that is positioned in proximity to the conjunctiva of the limbal region. (**B**) Treated eye. *Open arrows*: borderlines of an episcleral vein. A fibrous proliferation was evident that almost completely obstructed the venous lumen. C, conjunctival epithelium; CB, ciliary body; S, sclera; EV, episcleral vein lumen. Bar, 50 μm.

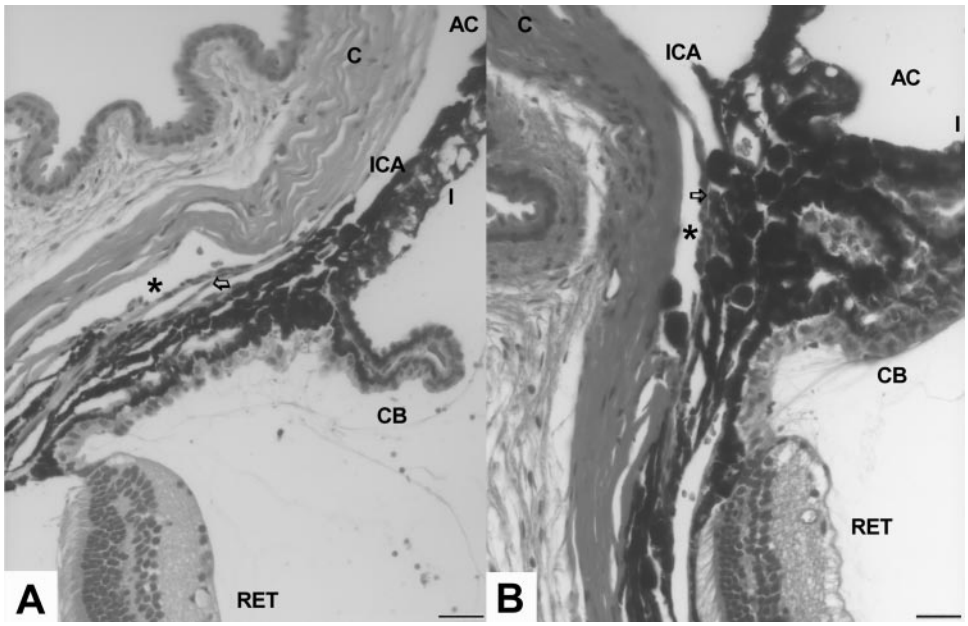

FIGURE 8. (**A**) Histology of the anterior segment in a control eye. *Arrow*: epithelial lining of the trabecular meshwork; (⋆) Schlemm's canal lumen. (**B**) Histology of the anterior segment of the surgical eye (60 days after surgery). Partial obstruction of Schlemm's canal was detectable (⋆), and the trabecular meshwork structure was completely destroyed and obstructed (*arrow*). Outer segments and retinal pigment epithelium of the peripheral retina did not have signs of damage induced by direct application of the diode laser. AC, anterior chamber; C, cornea; CB, ciliary body; I, iris; ICA, iridocorneal angle; RET, peripheral retina. Bar, 50 μm.

we analyzed ERG amplitudes (a- and b-waves) from mice that received indocyanine green injection but not laser treatment ($n = 5$) and mice that received laser treatment only ($n = 4$). An indocyanine green injection did not cause decrease of a-wave ($P = 0.6$, paired *t*-test) or b-wave ($P = 0.2$, paired *t*-test) amplitudes 3 weeks after surgery. Mice that received only laser treatment did not show ERG deficits in surgical eyes compared with control (nonsurgical) eyes 3 weeks after surgery (a-wave amplitudes, $P = 0.34$; b-wave amplitudes, $P = 0.16$, paired *t*-test).

Correlation Analysis of Tonometry and ERG Data

Detailed analysis of tonometry and electroretinography data revealed significant correlation between ocular hypertension expressed as a coefficient of IOP elevation and ERG amplitudes: $(IOP_{surgical\ eyes} - IOP_{control\ eyes}) \times$ duration of hypertension (mm Hg × days) versus ERG amplitudes expressed as a ratio (surgical/control, %).

Correlation analysis data were IOP versus a-wave ($r^2 = 0.2$; $P = 0.0002$), IOP versus b-wave ($r^2 = 0.4$; $P < 0.0001$), and IOP versus OPs ($r^2 = 0.2$; $P = 0.0004$). Analysis did not reveal significant correlation between IOP and flERG amplitudes ($r^2 = 0.02$; $P = 0.18$).

Histologic Analysis

Our electrophysiological studies revealed a reduction of the function in all retinal layers. Histologic analysis was performed to determine whether functional defects were in agreement with the morphologic appearance of the surgical eyes.

Light microscopy analysis revealed an obstruction of the episcleral veins (Fig. 7), trabecular meshwork destruction with partial or complete obstruction of Schlemm's canal (Fig. 8), and development of anterior synechia in nine surgical eyes (Fig. 10A). The thickness of all retinal layers appeared decreased in surgical eyes compared with the control (Fig. 10E). Light microscopy analysis of optic nerves revealed moderate to extensive damage of optic nerve structures (Fig. 11).

Electron microscopy analysis of the optic nerves (Fig. 12) revealed loss and degeneration (electron-dense appearance, Fig. 12B) of the large diameter axons, swelling of myelin sheaths, condensation and degeneration of the cytoskeleton (Fig. 12C), and activation of the glial cells in proximity to degenerating axons (Fig. 12C–F).

For the analysis, we compared measurement of the thickness of the IPL and RGC layer (IPL+RGC), INL, and ONL, and total retinal thickness between control and surgical eyes (Table 1). Morphometric analysis revealed significant reduction of the total retinal thickness. However, a separate analysis of the ONL, INL, and IPL+RGC layers in surgical eyes did not reveal statistically significant thinning compared with control (nonsurgical) eyes.

Correlation Analysis of Histology and ERG Data

Linear regression analysis revealed poor correlation between OP amplitudes and combined retinal thickness of the RGC and IPL layers, expressed as a ratio between surgical and control eyes ($r^2 = 0.09$, $P = 0.6$). Calculated correlation coefficients did not reveal significant correlations between morphologic and functional analysis for other retinal layers: a-wave ratio versus ONL thickness ($r^2 = 0.15$, $P = 0.09$), b-wave ratio

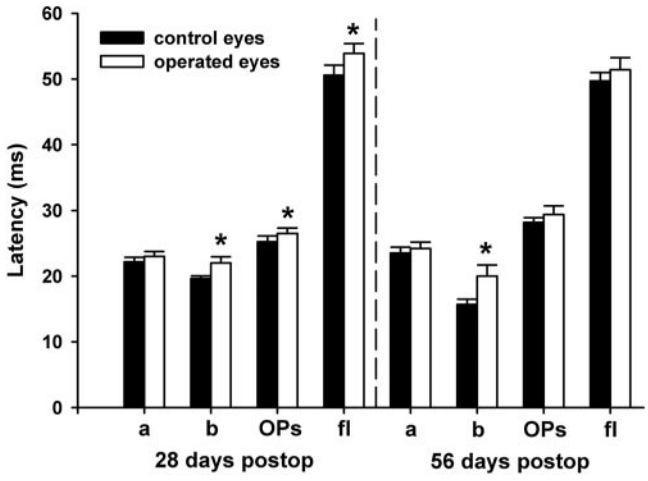

FIGURE 9. Latency analysis for different ERG components. a, a-wave latency; b, b-wave latency; OPs, oscillatory potentials latency; fl, flicker ERG latency. $^*P < 0.05$.

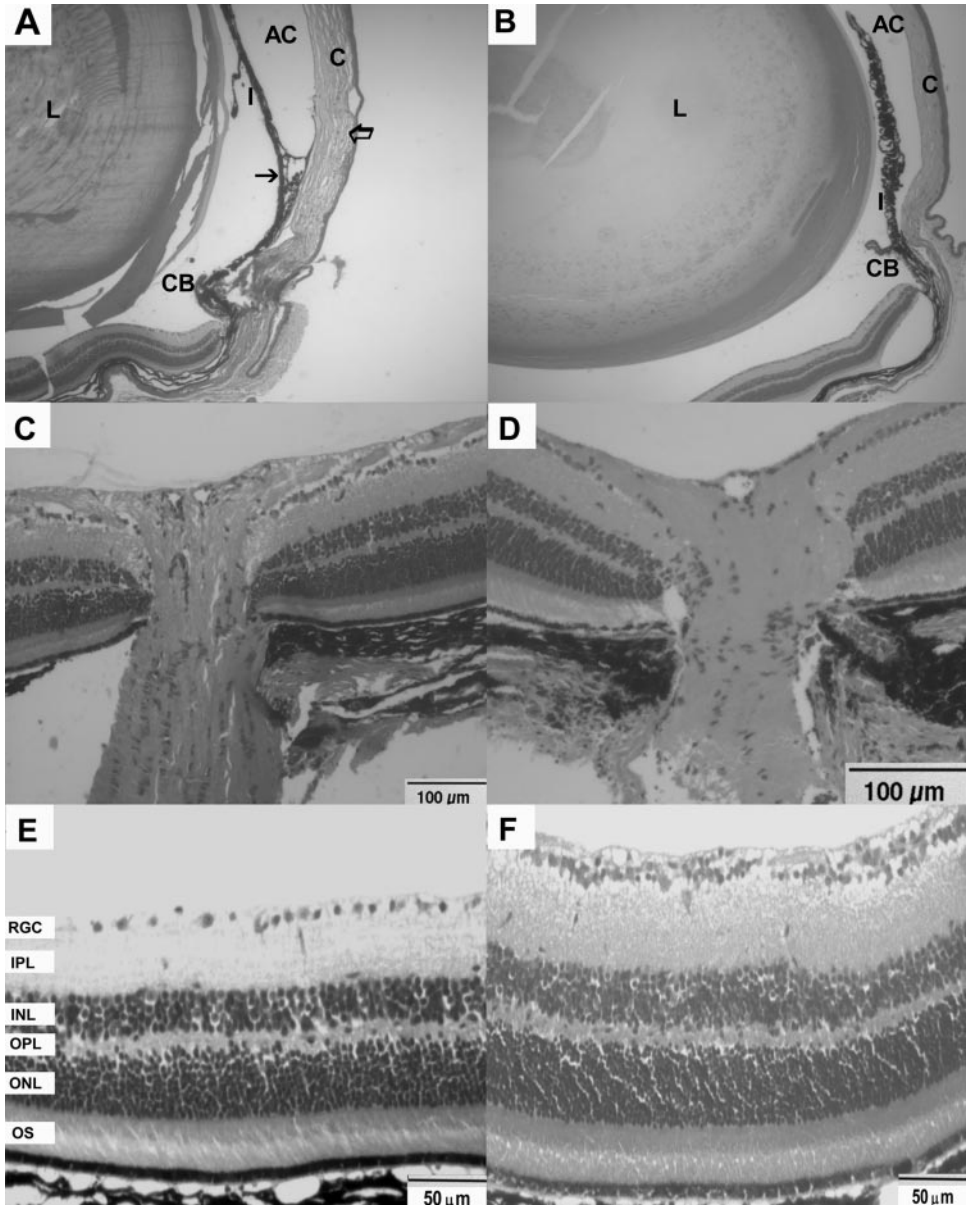

FIGURE 10. Light microscopy of surgical (**A**, **C**, **E**) and control (**B**, **D**, **F**) eyes. Surgical eyes were characterized by development of trabecular meshwork destruction with partial or complete obstruction of Schlemm's canal, whereas a minority of eyes ($n = 9$) had detectable development of the anterior synechia. Optic nerve head distortion, without evidence of prominent cupping and decreased thickness of the retina with a loss of RGCs were major features of surgical eyes. Laser-induced damage to the peripheral retina (uveitis, retinal detachment, RPE, and photoreceptor destruction) was not detected by light microscopy. AC, anterior chamber; C, cornea; CB, ciliary body; I, iris; OPL, outer plexiform layer; OS, outer segments. *Arrow*: corneal edema.

versus INL thickness ($r^2 = 0.13$, $P = 0.1$) and b-wave ratio versus IPL+RGC layer thickness ($r^2 = 0.03$, $P = 0.42$).

DISCUSSION

The experimental approach used in this study allowed the precise monitoring of the dynamics of retinal damage during chronic elevation of IOP. Laser cauterization of the indocyanine green–pretreated eyes was a successful procedure for the induction of chronic elevation of IOP in mouse eyes. Laser-induced cauterization caused rapid elevation of IOP during the first 12 hours of the postoperative period (34 mm Hg), which was sustained for at least 4 weeks.

Analysis of the ERG parameters (amplitudes and latency of scotopic flash ERG, OPs, and flERG) was an effective strategy for the functional monitoring of different cell populations in the retina. Previous reports have indicated that recording the OPs may be a relatively sensitive method to detect retinal damage in glaucomatous eyes.[30,31] Our results show that, indeed, OPs were the most dramatically affected in chronically hypertensive mouse eyes. Chronic hypertension in the mice also affected a- and b-wave components of the scotopic flash ERG. Similar type of changes have been reported in a study that observed ERG changes in DBA/NNi mice, which undergo development of spontaneous glaucoma.[32,33] Detailed analysis of the pattern ERG responses in DBA/2NNi mice revealed development of significant functional deficits as early as 5 months of age.[32] An ERG analysis of scotopic flash ERG amplitudes revealed development of significant a-wave deficits by 7 months of age, whereas b-wave deficits were detected at 8 months of age.[33] It has been reported that DBA mice have the maximum elevation of IOP at the age of 9 months (20.3 mm Hg),[34] which corresponds to the development of significant ERG deficits,[33] and thus it was not unexpected to observe similar ERG deficits in our model, because elevation of IOP was present immediately after surgery in ranges that were much higher than in DBA mice. Because mice do not have a developed lamina cribrosa,[35] there is a possibility that damage induced by elevation of IOP is distributed not only to the optic nerve but also to the different retinal layers. Functional analysis of the sham-operated mice that received only laser treatment or indocyanine green injection did not reveal functional deficits com-

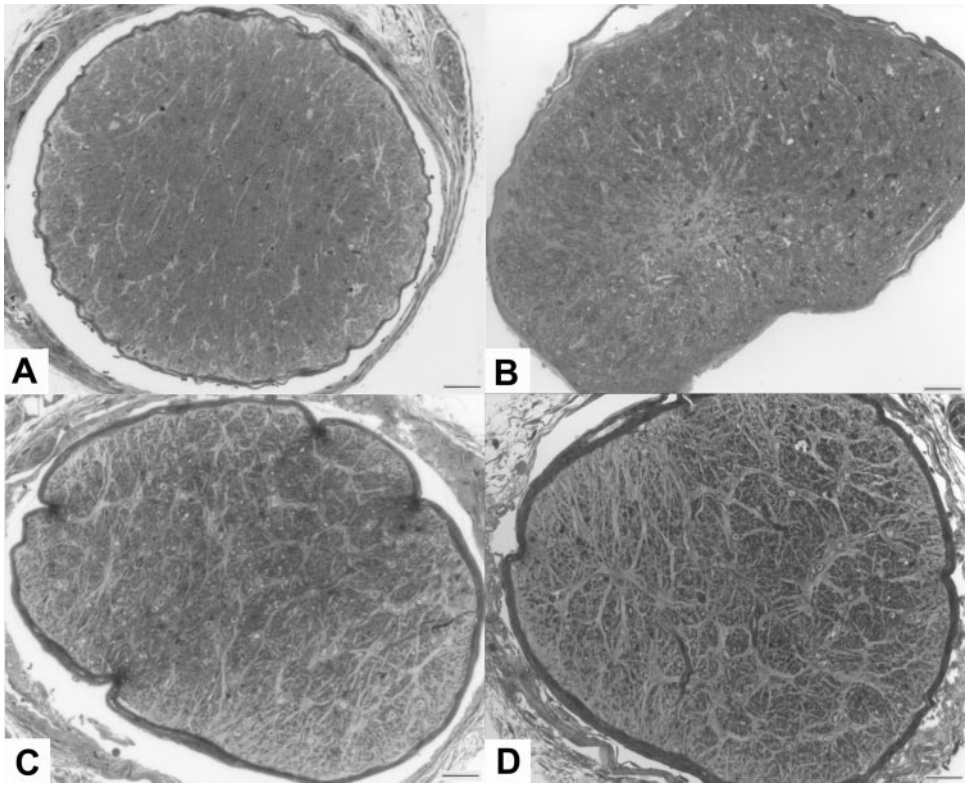

FIGURE 11. Light microscopy analysis of optic nerves revealed different levels of damage. (**A**) Control; (**B–D**) surgical eyes. Massive degeneration of the optic nerves was evident. Bar, 100 μm.

pared with the control eyes, which rules out the possibility that invasive manipulation of the eyes and/or laser energy are responsible for the detected functional deficits. Furthermore, detailed histologic analysis of peripheral retinas in surgical eyes, which received combined treatment (indocyanine green injection and laser application) did not reveal uveitis, retinal detachment, destruction of the retinal pigment epithelium, or photoreceptors in proximity to the trabecular meshwork, where the effect of direct laser energy should be the most extensive.

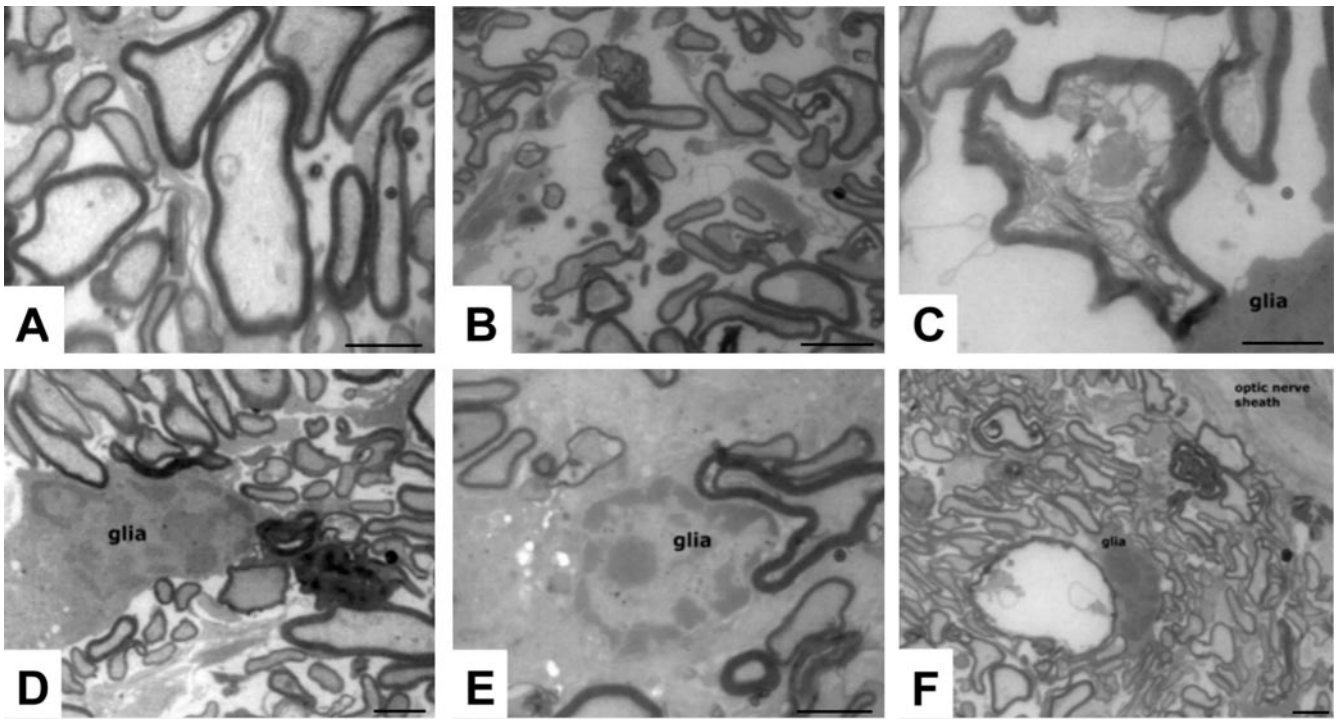

FIGURE 12. Electron microscopy analysis of optic nerves of the control (**A**) and surgical (**B–F**) eyes. Degeneration of large diameter axons and gliosis were the most predominant features in the optic nerves of the surgical eyes. (**E**) Gliosis of the optic nerve in the surgical eye. Scale bars: (**A**, **C**, **E**) 500 nm; (**B**, **D**, **F**) 1 μm.

TABLE 1. Morphometric Analysis of the Retina

	IPL + RGC	INL	ONL	Total Thickness
Control	36.9 ± 1.2	25.5 ± 0.9	47.5 ± 1	109.9 ± 2.4
Surgical	34.5 ± 1.9	23.9 ± 1	45.3 ± 1.2	103.7 ± 3.5*

Data are mean micrometers ± SEM.
* $P < 0.05$; paired *t*-test.

Histologic and electron microscopy analysis data revealed damage of the optic nerve and thinning of all retina layers. Detailed examination of the anterior chambers in surgical eyes revealed complete destruction of the trabecular meshwork, complete or partial obstruction of Schlemm's canal, and development of anterior synechia that were probably responsible for the decreased aqueous humor outflow and elevated IOP that were the final result. However, we cannot exclude the possibility that photocoagulation of episcleral veins did not participate at least partially in the development of chronic ocular hypertension.

Probably the most interesting models of glaucoma in recent years have been mouse models in which chronic ocular hypertension develops: DBA/2NNia, DBA/2J, and AKXD-28/Ty mice.[32,34,36] However, the small size of the eye and difficulties in obtaining IOP data have partially diminished the more frequent use of these animals in glaucoma studies.

DBA/2 inbred mouse strains have been found to exhibit spontaneous development of a form of a secondary glaucoma phenotype: pigment-dispersion glaucoma.[33,34,36] The exact genetic defect responsible for the DBA/2J (D2) phenotype was recently identified.[37] Using mapping techniques, sequencing, and functional genetic tests, Anderson et al.[37] showed that iris pigment dispersion (IPD) and iris stromal atrophy (ISA) result from mutations in related genes encoding melanosomal proteins (*Gpnmb* and *TYRP1*). They hypothesized that IPD and ISA alter melanosomes, allowing toxic intermediates of pigment production to leak from melanosomes, causing iris disease and subsequent pigmentary glaucoma. However, a recent study[38] did not identify mutation of the *TYRP1* gene in humans with pigmentary glaucoma.

Although models of spontaneous development of glaucoma have considerable value for glaucoma research, inducible models have the unique advantage of providing control parameters from the same animal (one eye surgically treated and the fellow eye as the control) with the dramatically increased speed of data generation from different transgenic lines.

Understanding glaucoma pathophysiology depends on the precise correlation of molecular events and in vivo changes in retinal and optic nerve function during the progression of the disease. An objective estimation of retinal and optic nerve function can be achieved by recording ERG (flash, flicker, OPs), visual evoked potentials (VEPs), and the pupil light reflex (PLR). The characterization of the ERG amplitudes and latencies are likely to have significant importance in the evaluation of precise localization of the retinal damage due to chronic ocular hypertension in mouse eyes. We have recently demonstrated that laser surgery in mouse eyes results in the development of PLR and ERG deficits (Grozdanic S, et al. *IOVS* 2002; 43:ARVO E-Abstract 4033). Because strategies for the induction of retinal and optic nerve damage due to elevated IOP involve surgery on one eye, simultaneous monitoring of physiological function in surgical and nonsurgical eyes may provide precise information about development of functional deficits. Furthermore, the procedure of inducing increased IOP in one eye allows collection of control tissue (nonsurgical eye) from the same animal, which may reduce the number of animals to be used in experiments and decrease data variability. This relatively straightforward procedure for the induction of ocular hypertension may provide a unique opportunity for the use of different transgenic animals without any limitations and in a relatively short period. Such approach may offer extensive opportunities to test different hypotheses about the involvement of the different molecular mechanisms that may be responsible for glaucomatous neuropathy.

CONCLUSION

A mouse model of laser-induced chronic ocular hypertension for studying glaucoma may have the potential to become a powerful experimental tool in the development of neuroprotective drugs and molecular determination of the pathogenesis of glaucoma.

Acknowledgments

The authors thank Haag-Streit USA, Inc., and Rolf Pfister for providing the mouse measuring prism and modification of the Goldmann tonometer.

References

1. Quigley HA. Neuronal death in glaucoma. *Prog Retinal Eye Res.* 1999;18:39–57.
2. Leske MC. The epidemiology of open-angle glaucoma: a review. *Am J Epidemiol.* 1983;118:166–191.
3. Allen RC. Medical management of glaucoma. In: Albert DM, Jakobiec FA, eds. *Principles and Practice of Ophthalmology.* 2nd ed. Philadelphia, PA: WB Saunders; 2000:2891–2916.
4. Craig J, Mackey D. Glaucoma genetics: where are we? Where will we go? *Cur Opin Ophthalmol.* 1999;10:126–134.
5. Liu B, Neufeld AH. Expression of nitric oxide synthase-2 (NOS-2) in reactive astrocytes of the human glaucomatous optic nerve head. *Glia.* 2000;30:178–186.
6. Neufeld AH, Hernandez MR, Gonzalez M. Nitric oxide synthase in the human glaucomatous optic nerve head. *Arch Ophthalmol.* 1997;115:497–503.
7. Neufeld AH, Sawada A, Becker B. Inhibition of nitric oxide synthase-2 by aminoguanidine provides neuroprotection of retinal ganglion cells in a rat model of chronic glaucoma. *Proc Natl Acad Sci USA* 1999;96:9944–9948.
8. Yan X, Tezel G, Wax MB, Edward DP. Matrix metalloproteinases and tumor necrosis factor alpha in glaucomatous optic nerve head. *Arch Ophthalmol.* 2000;118:666–673.
9. Tezel G, Li LY, Patil RV, Wax MB. TNF-alpha and TNF-alpha receptor-1 in the retina of normal and glaucomatous eyes. *Invest Ophthalmol Vis Sci.* 2001;42:1787–1789.
10. Pease ME, McKinnon SJ, Quigley HA, Kerrigan-Baumrind LA, Zack DJ. Obstructed axonal transport of BDNF and its receptor TrkB in experimental glaucoma. *Invest Ophthalmol Vis Sci.* 2000;41:764–774.
11. Pena JD, Agapova O, Gabelt BT, et al. Increased elastin expression in astrocytes of the lamina cribrosa in response to elevated intraocular pressure. *Invest Ophthalmol Vis Sci.* 2001;42:2303–231.
12. Hayreh SS. The role of age and cardiovascular disease in glaucomatous optic neuropathy. *Surv Ophthalmol.* 1999;43(suppl 1): S27–S42.
13. Duijm HFA, Thomas J, van de Berg TP, Greve EL. Comparison of retinal and choroidal hemodynamics in patients with primary open-angle glaucoma and normal-pressure glaucoma. *Am J Ophthalmol.* 1997;123:644–656.
14. Yamazaki Y, Drance SM. The relationship between progression of visual field defects and retrobulbar circulation in patients with glaucoma. *Am J Ophthalmol.* 1997;124:287–295.
15. Caballero M, Borras T. Inefficient processing of an olfactomedin-deficient myocilin mutant: potential physiological relevance to glaucoma. *Biochem Biophys Res Commun.* 2001;282:662–670.

16. Goldblum D, Mittag T. Prospects for relevant glaucoma models with retinal ganglion cell damage in the rodent eye. *Vision Res*. 2002;42:471–478.
17. Levkovitch-Verbin H, Harris-Cerruti C, Groner Y, Wheeler LA, Schwartz M, Yoles E. RGC death in mice after optic nerve crush injury: oxidative stress and neuroprotection. *Invest Ophthalmol Vis Sci*. 2000;41:4169–4174.
18. Bayer AU, Keller ON, Ferrari F, Maag KP. Association of glaucoma with neurodegenerative diseases with apoptotic cell death: Alzheimer's disease and Parkinson's disease. *Am J Ophthalmol*. 2002; 133:135–137.
19. Copin B, Brezin AP, Valtot F, Dascotte JC, Bechetoille A, Garchon HJ. Apolipoprotein E-promoter single-nucleotide polymorphisms affect the phenotype of primary open-angle glaucoma and demonstrate interaction with the myocilin gene. *Am J Hum Genet*. 2002;70:1575–1581.
20. Vickers JC, Craig JE, Stankovich J, et al. The apolipoprotein epsilon4 gene is associated with elevated risk of normal tension glaucoma. *Mol Vis*. 2002;8:389–393.
21. Grozdanic S, Torres MI, Betts DM, et al. Characterization of aqueous humor flow and pupil light reflex in the mouse: applications for development of a mouse model of glaucoma. Presented at the Annual Meeting of the American College of Veterinary Ophthalmologists, Sarasota, Florida, 2001.
22. Grozdanic S, Betts DM, Allbaugh RA, et al. Characterization of the pupil light reflex, electroretinogram and tonometric parameters in healthy mouse eyes. *Curr Eye Res.* 2003;26:371–378.
23. Chew SJ. Animal models of glaucoma. In: Ritch R, Shields MB, Krupin T, eds. *The Glaucomas*: *Basic Sciences, Anatomy and Pathology.* Vol. 1. 2nd ed. New York: Mosby, 1996:55–70.
24. Ueda J, Sawaguchi S, Hanyu T, et al. Experimental glaucoma model in the rat induced by laser trabecular photocoagulation after an intracameral injection of India Ink. *Jpn J Ophthalmol*. 1998;42: 337–344.
25. Cohan BE, Bohr DF. Measurement of intraocular pressure in awake mice. *Invest Ophthalmol Vis Sci*. 2001;42:2560–2562.
26. Goldmann H. Abflussdruck minutenvolumen und widerstand der Kammerwasser Stromung des Menschen. *Doc Ophthalmol.* 1951; 5–6:278–356.
27. Toris C, Zhan G, Wang Y, et al. Aqueous humor dynamics in monkeys with laser-induced glaucoma. *J Ocul Pharm Ther.* 2000; 16:19–27.
28. Larsson L. Aqueous humor flow in normal human eyes treated with brimonidine and timolol, alone and in combination. *Arch Ophthalmol.* 119:492–495, 2001.
29. Grozdanic S, Sakaguchi DS, Kwon YH, Kardon RH, Sonea IM. Functional characterization of retina and optic nerve after acute ocular ischemia in rats. *Invest Ophthalmol Vis Sci.* 2003;44:2597–2605.
30. Gur M, Zeevi YY, Bielik M, Neumann E. Changes in the oscillatory potentials of the electroretinogram in glaucoma. *Curr Eye Res*. 1987;6:457–466.
31. Fortune B, Bearse MA Jr, Cioffi GA, Johnson CA. Selective loss of an oscillatory component from temporal retinal multifocal ERG responses in glaucoma. *Invest Ophthalmol Vis Sci*. 2002;43:2638–2647.
32. Bayer AU, Brodie SE, Mittag T. Pilot study of pattern-electroretinographic changes in the DBA/2NNia mouse: animal model of congenital angle-closure glaucoma. *Ophthalmologe*. 2001;98:248–252.
33. Bayer AU, Neuhardt T, May AC, et al. Retinal morphology and ERG response in the DBA/2NNia mouse model of angle-closure glaucoma. *Invest Ophthalmol Vis Sci*. 2001;42:1258–1265.
34. John S, Smith R, Savinova O, et al. Essential iris atrophy, pigment dispersion, and glaucoma in DBA/2J mice. *Invest Ophthalmol Vis Sci.* 1998;39:951–962.
35. May CA, Lütjen-Drecoll E. Morphology of the murine optic nerve. *Invest Ophthalmol Vis Sci*. 2002;43:2206–2212.
36. Anderson M, Smith R, Savinova O, et al. Genetic modification of glaucoma associated phenotypes between AKXD-28/Ty and DBA/2J mice. *BMC Genetics*. 2001;2:1.
37. Anderson MG, Smith RS, Hawes NL, et al. Mutations in genes encoding melanosomal proteins cause pigmentary glaucoma in DBA/2J mice. *Nat Genet*. 2002;30:81–85.
38. Lynch S, Yanagi G, DelBono E, Wiggs JL. DNA sequence variants in the tyrosinase-related protein 1 (TYRP1) gene are not associated with human pigmentary glaucoma. *Mol Vis*. 2002;8:127–129.